# Donor−Acceptor-Type Low Bandgap Polymer Carrying Phenylazomethine Moiety as a Metal-Collecting Pendant Unit: Open-Circuit Voltage Modulation of Solution-Processed Organic Photovoltaic Devices Induced by Metal Complexation

Atsushi Kimoto* and Yusuke Tajima

Center for Intellectual Property Strategies, RIKEN, 2-1 Hirosawa, Wako 351-0198, Japan

Ⓢ *Supporting Information*

ABSTRACT: A novel low-bandgap conjugated polymer with the phenylazomethine moiety as a pendant metal-collecting unit (PImCDTBT) was synthesized via Suzuki cross-coupling copolymerization. Its basic physicochemical properties were revealed, and the optical bandgap and highest occupied molecular orbital (HOMO) energy levels were estimated to be 1.73 eV and −5.36 eV, respectively. PImCDTBT successfully assembles metal ions on its phenylazomethine site, as evidenced by a spectral change similar to that of its monomeric model compounds. In a bulk heterojunction photovoltaic device, the open-circuit voltage was clearly enhanced from 0.46 to 0.52 V by complexation of PImCDTBT, with only 1 wt % of $SnCl_2$. This was due to a change in either the electronic state of the polymer or its environment by complexing with the cationic Sn^{2+} ion.
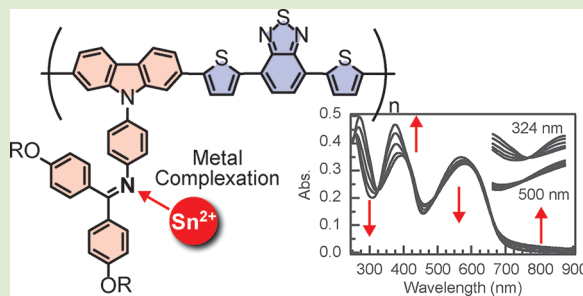
Investigations of solution-processed organic photovoltaic (OPV) devices, which are based on the bulk heterojunction strategy with the use of a π-conjugated polymer (electron donor) and a fullerene derivative (electron acceptor), have increased rapidly during the past decade.[1] To improve photoconversion efficiency, one of the most promising approaches is to broaden the light-absorbing property of the active layer and to improve the short circuit current (J_{SC}). Broad light absorption has been achieved on the basis of the intramolecular charge transfer (CT) transition between the electron-sufficient and electron-deficient backbone.[2] Nevertheless, the improvement of J_{SC} could be achieved more practically by annealing methods,[3] appropriate donor/acceptor mixing ratios,[4] and processing additives[5] to offer the ideal bulk heterojunction structure with a large donor/acceptor interfacial area. Another more important approach is to modulate the intrinsic electronic properties (highest occupied molecular orbital (HOMO) and lowest unoccupied molecular orbital (LUMO) energy levels) of the constituent electron donor[6] and acceptor[7] to improve the open circuit voltage (V_{OC}) of OPV devices by introducing electron-donating and/or electron-withdrawing substituents. For investigations in which these design strategies are integrated, π-conjugated polymers and fullerene derivatives consistently drive photovoltaic performance with high photoconversion efficiencies of up to 10%.[8] In parallel to the extension of established methodologies for novel building blocks, the cultivation of easily processable strategies for improving OPV characteristics by fundamentally tailoring the electronic state of the active layer would be of great importance. One practical approach is to employ interfacial dipole moments to align the energy levels at the heterojunction with a multilayered device structure, which results in the flexible adjustment of the V_{OC} of poly(3-hexylthiophene) (P3HT)/[6,6]-phenyl C_{61}-butyric acid methyl ester (PCBM) devices.[9]

Here, we focus on complexation in polyaniline[10] and phenylazomethine derivatives, which plays an important role in the improvement of various organic electronic devices such as organic electroluminescent devices[11] and dye-sensitized solar cells.[12] To incorporate this "complexation effect" into bulk heterojunction-type OPV devices, we designed a p-type donor−acceptor-type π-conjugated polymer possessing the pendant phenylazomethine moiety as a metal ligation site (PImCDTBT). We now report for the first time the application of metal complexation in phenylazomethine to the tuning of OPV parameters as an easily processable methodology for improving OPV performance with a single-layered device structure.

The phenylazomethine-appended monomer was prepared as shown in Scheme 1. The formation of the phenylazomethine backbone was followed by the dehydration reaction of aromatic ketone (**1**) with aromatic amine (**2**)[13] in the presence of titanium(IV) tetrachloride and 1,4-diazabicyclo[2.2.2]octane (DABCO) to give compound **3** in 90% yield.[14] Transformation of **3** under Miyaura borylation conditions furnished the key

Scheme 1. Synthesis of the Phenylazomethine-Appended Monomer, 4[a]
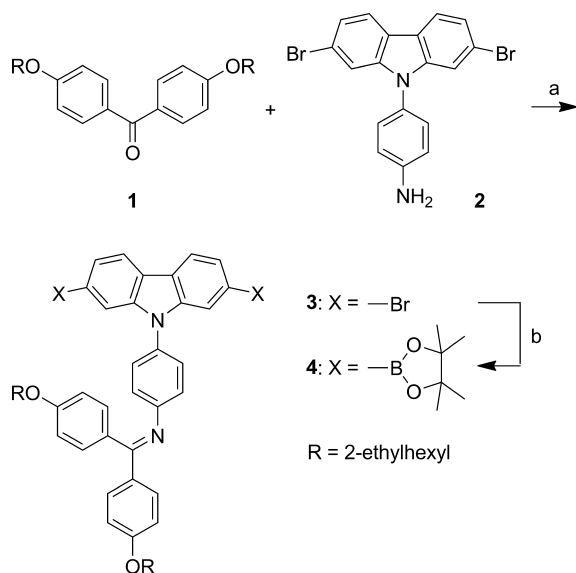
[a]Reagents and conditions: (a) TiCl$_4$, DABCO, PhCl; (b) bis-(pinacolato)diboron, potassium acetate, PdCl$_2$(dppf), 1,4-dioxane.

monomer **4** in 80% yield. The carbazole-based donor–acceptor-type copolymer bearing a phenylazomethine backbone (PImCDTBT) was prepared by the palladium-catalyzed Suzuki cross-coupling polymerization of **4** and **5** (Scheme 2). The

Scheme 2. Synthesis of PImCDTBT[a]
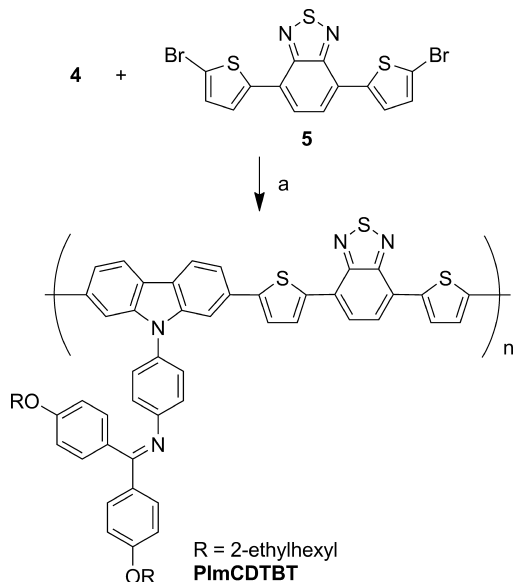
[a]Reagents and conditions: (a) Pd(PPh$_3$)$_4$, 2 M Na$_2$CO$_3$, Aliquat336, toluene.

molecular weight (M_w) and polydispersity (M_w/M_n) of the polymer, as determined by gel permeation chromatography (GPC) (eluent, *o*-dichlorobenzene), were 5300 and 2.12, respectively. The ^{1}H NMR spectrum exhibits a characteristic peak at around 4.0 ppm, which is attributed to the alkoxy proton derived from the solubilizing unit. This indicates the successful introduction of the phenylazomethine backbone. Considering an M_n is 2500, which corresponds to a degree of

polymerization of less than 3, the end groups should be readily visible in the NMR spectra. We compared the integration value of the alkoxy protons and that of the aromatic protons and estimated the degree of polymerization from the NMR spectrum. The integration ratio of signals (aromatic to alkoxy proton) is 8.4:1. Investigating the oligomer structure, we estimated that the oligomer has the structure with two **4** units and three **5** units with two phenyl ring as end-cap ($M_w = 2403$). Its integration ratio of signals (aromatic to alkoxy proton) is 8:1, which is reasonable value for experimental integration ratio. More details are described in the Supporting Information.

The normalized UV−vis absorption spectra of PImCDTBT in chlorobenzene and in the film state are shown in Figure 1a. A
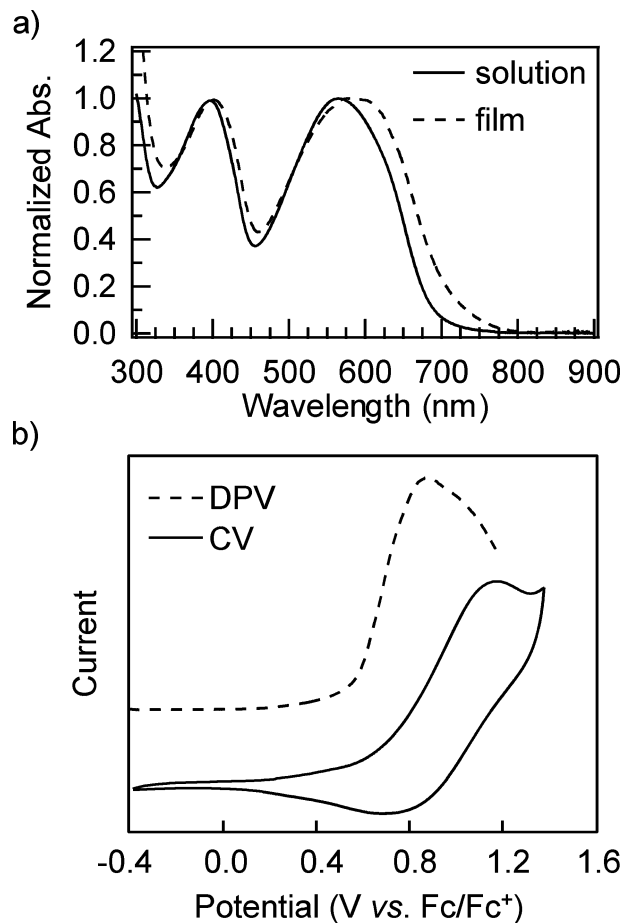

Figure 1. (a) UV−vis absorption spectra of PImCDTBT in chlorobenzene and film prepared by spin-coating from chlorobenzene solution (normalized at λ_{max} in the visible region). (b) Cyclic voltammogram and differential pulse voltammogram of the cast film of PImCDTBT measured in acetonitrile at a scan rate of 100 mV/s with Bu$_4$NPF$_6$ (0.1 mol/L) as the electrolyte. The film was prepared by spin-coating a chloroform solution on the working electrode.

characteristic absorption around 600 nm with a maximum (λ_{max}) at 584 nm is attributed to the intramolecular CT transition between the electron-rich phenylcarbazole and electron-deficient benzothiadiazole units. In the solid state, PImCDTBT showed a significant red shift with a λ_{max} of 603 nm. The optical bandgap is 1.73 eV, as estimated from the absorption onset (715 nm). The electrochemical properties of PImCDTBT were studied by cyclic voltammetry (Figure 1b). The HOMO values are determined from the onset values of

oxidation potential with respect to ferrocene (Fc) (4.8 eV below the vacuum level). PImCDTBT displayed oxidation waves attributed to the oxidation of the carbazole unit. From the cyclic voltammogram, we estimated the HOMO value to be −5.36 eV. Compared with the HOMO energy level of other carbazole-based low bandgap polymers, this value is reasonable and appropriate for photovoltaic devices with the standard configuration. From the optical bandgap, the LUMO energy level was estimated to be −3.63 eV.

With the addition of $SnCl_2$[15] to the chloroform/acetonitrile solution of PImCDTBT and its monomers, the absorption spectrum of PImCDTBT changed in a way similar to that of **4** (Figures 2 and S9 and S10a of the Supporting Information),
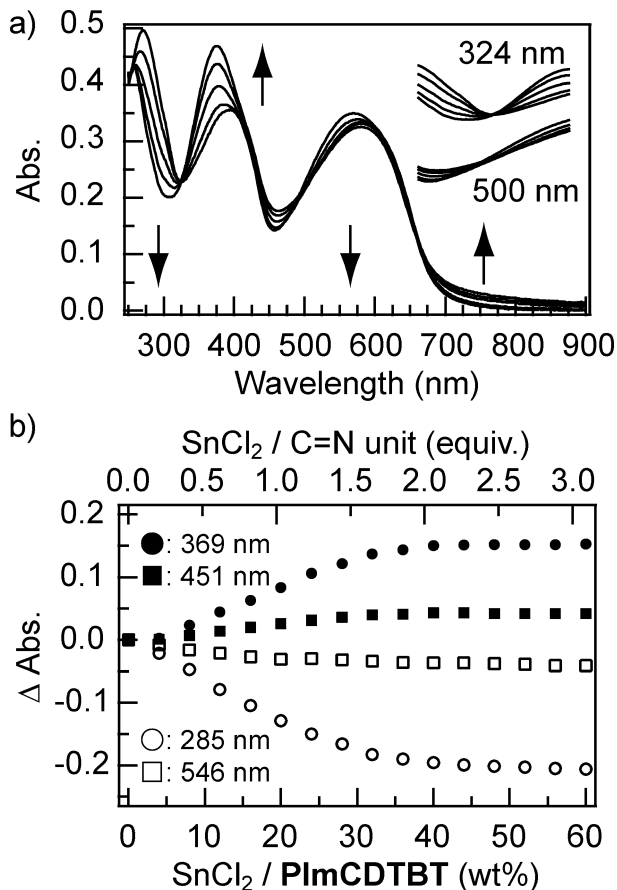

Figure 2. (a) UV−vis spectral changes of PImCDTBT (inset). Enlargements focusing on isosbestic points and (b) titration curve on stepwise addition of $SnCl_2$ in $CH_3CN/CHCl_3$ = 1:4.

whereas no drastic spectral changes were observed for 4,7-dithien-5′-yl-2,1,3-benzothiadiazole (Figure S10b).[16] Considering that only a small spectral change in the absorption band attributed to the CT transition between the carbazole and benzothiadiazole is observed, the electronic state of PImCDTBT is similar even during complexation with the cationic Sn^{2+} ion. These results suggest that the complexation reaction occurs only at the pendant phenylazomethine site in PImCDTBT. In addition, they suggest that there is only a slight change in the electronic state in the carbazole unit via complexation,[17] consistent with the results obtained via electrochemical measurements; almost the same redox behavior was observed for PImCDTBT complexed with an equimolar amount of $SnCl_2$ for one phenylazomethine unit (Figure

S11).[18,11b] During the complexation reaction with $SnCl_2$, the absorption spectrum showed three characteristic isosbestic nodes (324, 500, and 665 nm) in the visible region (>300 nm) for complexation on the phenylazomethine moiety.[19] These representative spectral changes, which are similar to those of the model compound, support the result that the complexation of $SnCl_2$ occurs at the phenylazomethine unit beside the polymers. Considering that the equilibrium constant for the formation of 1:1 complexes with $SnCl_2$ on the imine sites was estimated to be around 10^5 (M^{-1}),[20] the saturated spectral changes after adding 1.5 equiv for one phenylazomethine unit (Figure 2b) are also reasonable for complexation exclusively on the phenylazomethine site.

Bulk heterojunction-type OPV devices were preliminarily fabricated with the device structure of ITO/PEDOT:PSS/PImCDTBT:PCBM (1:3, w:w)/Al [where ITO is indium tin oxide and PEDOT:PSS is poly(3,4-ethylenedioxythiophene) poly(styrenesulfonate)] is to verify the effect of metal complexation on the p-type π-conjugated polymer. The devices were measured under the simulated AM 1.5 G illumination condition (100 mW/cm²). The device characteristics and current density−voltage curves are shown in Tables S1 and S2 and Figure 3. For the best device, clearly, the V_{OC} was enhanced
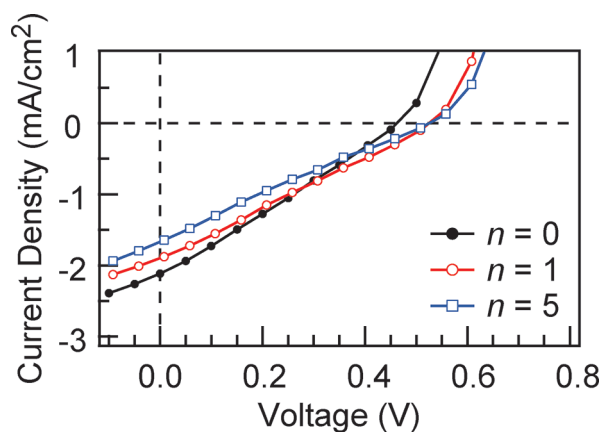

Figure 3. Current density−voltage (J−V) curves. Device configuration: ITO/PEDOT:PSS/PImCDTBT + n wt % $SnCl_2$ complex:PCBM (1:3, w:w)/Al.

from 0.46 to 0.52 V through the complexation of PImCDTBT with 1 wt % of $SnCl_2$. In contrast, the V_{OC} remained the same (0.52 V) by using PImCDTBT with 5 wt % of $SnCl_2$. The similar metal complexation effect can be confirmed for the average device characteristics for eight different devices. This increased V_{OC} by complexing with only 1 wt % (0.05 equiv for one phenylazomethine unit) of $SnCl_2$ implies that there is no relationship between the complexation-induced V_{OC} increase and the electronic state of PImCDTBT, especially of the carbazole unit. One possible reason for the "metal complexation effect" occurring only for complexation with 1 wt % of $SnCl_2$ is a change in the electronic properties of the active layer; that is, the environment around PImCDTBT is drastically tuned by incorporating $SnCl_2$, which has a high polarity and a large dipole moment. Modulating the dipole moment in the active layer induced by the incorporation of $SnCl_2$ might change the energy level gap between HOMO of the electron donor and LUMO of the electron acceptor, which results in the increase in V_{OC}. In contrast, the J_{SC} and fill factor (FF) decreased, resulting in a similar photoconversion efficiency

owing to the existence of ionic species that cause current leakage in the device.[21] Indeed, the use of PImCDTBT complexed with 5 wt % of SnCl$_2$ as the p-type polymer gives a lower J_{SC} and FF, despite the identical V_{OC} compared with the device based on PImCDTBT with 1 wt % of SnCl$_2$. Further efforts to optimize the device structure and amount of metal ion additive to improve J_{SC} and FF are currently ongoing.

In summary, a donor–acceptor-type π-conjugated polymer carrying the phenylazomethine moiety as a metal complexation site was synthesized and found to serve an important role in improving the characteristics of OPV devices. Complexation with a Lewis acid such as SnCl$_2$ enhances the V_{OC} values derived from a change in the electronic state of the active layer. The role of the phenylazomethine backbone is to collect the metal ions and to prevent the phase separation and formation of aggregates of SnCl$_2$ with large polarity. Advanced studies of device fabrication based on these polymers are currently under way. However, we believe that this simple methodology can be applied to obtain V_{OC} values (i.e., photoconversion efficiencies) beyond a theoretical limit without adopting multilayered device configurations.

■ EXPERIMENTAL METHODS

PImCDTBT–SnCl$_2$ complexes were prepared by the following method. To a solution of PImCDTBT in chloroform was added a solution of SnCl$_2$ in acetonitrile, and the mixture was evaporated to dryness to give the PImCDTBT complexes.

The polymers (PImCDTBT + n wt % SnCl$_2$ complex) and fullerene acceptors were codissolved in the solvent with a polymer concentration of 4 mg/mL at 40 °C for 12 h. The ITO-coated glass substrate was cleaned stepwise in water, acetone, and isopropyl alcohol under ultrasonication for 10−30 min each, after which it was dried in an oven. The ITO was subsequently cleaned with ozone. A thin layer (∼30 nm) of PEDOT:PSS (Baytron P VP A1 4083) was spin-coated onto the ITO surface. After being baked at 120 °C for ∼20 min, the substrates were transferred into a nitrogen filled glovebox. A ca. 40-nm-thick polymer/PCBM composite layer was then cast from the blend solution at 800−1200 rpm onto the ITO/PEDOT:PSS substrate and dried in vacuo for 30 min. The substrate was then transferred into a thermal evaporator located in the same glovebox. The Al layer (80 nm) was deposited, and the device was annealed at 80 °C for 10 min. The effective area was measured to be 6 mm^2. Device characterization was carried out under AM 1.5 G irradiation at the intensity of 100 mW/cm^2. Current density-versus-potential (J–V) curves were recorded with a Keithley 2400 digital sourcemeter.

■ ASSOCIATED CONTENT

ⓢ Supporting Information

Detailed experimental procedures and full characterization data for monomers and PImCDTBT. This material is available free of charge via Internet at http://pubs.acs.org.

■ AUTHOR INFORMATION

Corresponding Author

*E-mail: a_kimoto@riken.jp.

Notes

The authors declare no competing financial interest.

■ ACKNOWLEDGMENTS

■ REFERENCES

(1) (a) Padinger, F.; Rittberger, R.; Sariciftci, N. S. *Adv. Funct. Mater.* **2003**, *13*, 85−88. (b) Günes, S.; Neugebauer, H.; Sariciftci, N. S. *Chem. Rev.* **2007**, *107*, 1324−1338.

(2) (a) Cheng, Y. J.; Yang, S. H.; Hsu, C. S. *Chem. Rev.* **2009**, *109*, 5868−5923. (b) Boudreault, P. L. T.; Najari, A.; Leclerc, M. *Chem. Mater.* **2011**, *23*, 456−469. (c) Zhou, H.; You, W. *Macromolecules* **2012**, *45*, 607−632.

(3) (a) Ma, W.; Yang, C.; Gong, X.; Lee, K.; Heeger, A. J. *Adv. Funct. Mater.* **2005**, *15*, 1617−1622. (b) Li, G.; Shrotriya, V.; Huang, J.; Yao, Y.; Moriarty, T.; Emery, K.; Yang, Y. *Nat. Mater.* **2005**, *4*, 864−868. (c) Li, G.; Yao, Y.; Yang, H.; Shrotriya, V.; Yang, G.; Yang, Y. *Adv. Funct. Mater.* **2007**, *17*, 1636−1644.

(4) Park, S. H.; Roy, A.; Beaupré, S.; Cho, S.; Coates, N.; Moon, J. S.; Moses, D.; Leclerc, M.; Lee, K.; Heeger, A. J. *Nat. Photonics* **2009**, *3*, 297−303.

(5) (a) Peet, J.; Kim, J. Y.; Coates, N. E.; Ma, W. L.; Moses, D.; Heeger, A. J.; Bazan, G. C. *Nat. Mater.* **2007**, *6*, 497−500. (b) Lee, K.; Ma, W.; Brabec, C. J.; Yuen, J.; Moon, J. S.; Kim, J. Y.; Lee, K.; Bazan, G. C.; Heeger, A. J. *J. Am. Chem. Soc.* **2008**, *130*, 3619−3623.

(6) (a) Liang, Y.; Feng, D.; Wu, Y.; Tsai, S. T.; Li, G.; Ray, C.; Yu, L. *J. Am. Chem. Soc.* **2009**, *131*, 7792−7799. (b) Zhou, H.; Yang, L.; Stuart, A. C.; Price, S. C.; Liu, S.; You, W. *Angew. Chem., Int. Ed.* **2011**, *50*, 2995−2998.

(7) (a) Wienk, M. M.; Kroon, J. M.; Verhees, W. J. H.; Knol, J.; Hummelen, J. C.; van Hal, P. A.; Janssen, R. A. *Angew. Chem., Int. Ed.* **2003**, *42*, 3371−3375. (b) He, Y.; Chen, H. Y.; Hou, J.; Li, Y. *J. Am. Chem. Soc.* **2010**, *132*, 1377−1382.

(8) Green, M. A.; Emery, K.; Hishikawa, Y.; Warta, W.; Dunlop, E. D. *Prog. Photovolt: Res. Appl.* **2012**, *20*, 12−20.

(9) (a) Yuan, Y.; Reece, T. J.; Sharma, P.; Poddar, S.; Ducharme, S.; Gruverman, A.; Yang, Y.; Huang, J. *Nat. Mater.* **2011**, *10*, 296−302. (b) Tada, A.; Geng, Y.; Wei, Q.; Hashimoto, K.; Tajima, K. *Nat. Mater.* **2011**, *10*, 450−455.

(10) (a) Kulszewicz-Bajer, I.; Pron, A.; Abramowicz, J.; Jeandey, C.; Oddou, J. L.; Sobczak, J. W. *Chem. Mater.* **1999**, *11*, 552−556. (b) Genoud, F.; Kulszewicz-Bajer, I.; Bedel, A.; Oddou, J. L.; Jeandey, C.; Pron, A. *Chem. Mater.* **2000**, *12*, 744−749. (c) Genoud, F.; Kulszewicz-Bajer, I.; Dufour, B.; Rannou, P.; Pron, A. *Synth. Met.* **2001**, *119*, 415−416. (d) Higuchi, M.; Ikeda, I.; Hirao, T. *J. Org. Chem.* **1997**, *62*, 1072−1078. (e) Higuchi, M.; Imoda, D.; Hirao, T. *Macromolecules* **1996**, *29*, 8277−8279. (f) Hirao, T.; Higuchi, M.; Hatano, B.; Ikeda, I. *Tetrahedron Lett.* **1995**, *36*, 5925−5928. (g) Hirao, T.; Higuchi, M.; Ohshiro, Y.; Ikeda, I. *Chem. Lett.* **1993**, *22*, 1889−1890.

(11) (a) Satoh, N.; Cho, J. S.; Higuchi, M.; Yamamoto, K. *J. Am. Chem. Soc.* **2003**, *125*, 8104−8105. (b) Kimoto, A.; Cho, J. S.; Higuchi, M.; Yamamoto, K. *Macromolecules* **2004**, *37*, 5531−5537. (c) Albrecht, K.; Kasai, Y.; Kimoto, A.; Yamamoto, K. *Macromolecules* **2008**, *41*, 3793−3800. (d) Kimoto, A.; Cho, J. S.; Ito, K.; Aoki, D.; Miyake, T.; Yamamoto, K. *Macromol. Rapid Commun.* **2005**, *26*, 597−601. (e) Cho, J. S.; Kimoto, A.; Higuchi, M.; Yamamoto, K. *Macromol. Chem. Phys.* **2005**, *206*, 635−641. (f) Kimoto, A.; Masachika, K.; Cho, J. S.; Higuchi, M.; Yamamoto, K. *Chem. Mater.* **2004**, *16*, 5706−5712.

(12) (a) Satoh, N.; Nakashima, T.; Yamamoto, K. *J. Am. Chem. Soc.* **2005**, *127*, 13030−13038. (b) Nakashima, T.; Satoh, N.; Albrecht, K.; Yamamoto, K. *Chem. Mater.* **2008**, *20*, 2538−2543.

(13) Jian, H.; Tour, J. M. *J. Org. Chem.* **2003**, *68*, 5091−5103.

(14) (a) Williams, P. A.; Ellzey, K. A.; Padias, A. B.; Hall, H. K., Jr. *Macromolecules* **1993**, *26*, 5820−5821. (b) Higuchi, M.; Kimoto, A.; Shiki, S.; Yamamoto, K. *J. Org. Chem.* **2000**, *65*, 5680−5684.

(15) We selected SnCl$_2$ over other Lewis acids for initial trial, because (a) it is known that there is the formation of a 1:1 complex with phenylazomethine, and (b) there is no absorption in the visible region; it is easy to estimate the change in the bandgap of PImCDTBT, and we can exclude the absorption of the Lewis acid for OPV measurements.

(16) Kim, J. J.; Choi, H.; Lee, J. W.; Kang, M. S.; Song, K.; Kang, S. O.; Ko, J. *J. Mater. Chem.* **2008**, *18*, 5223−5229.

(17) In the literature, the complexation of strong Lewis acids on benzothiadiazole and its analogues in the main chain of π-conjugated polymers was reported, resulting in changes in the HOMO and LUMO energy levels with distinct spectral red shifts ($\Delta\lambda_{max} > 200$ nm for the CT transition absorption): (a) Welch, G. C.; Coffin, R.; Peet, J.; Bazan, G. C. *J. Am. Chem. Soc.* **2009**, *131*, 10802−10803. (b) Welch, G. C.; Bazan, G. C. *J. Am. Chem. Soc.* **2011**, *133*, 4632−4644.

(18) Additional stable redox waves attributed to the reduction of the azomethine-metal complex unit were not observed within the potential range.

(19) (a) Yamamoto, K.; Higuchi, M.; Shiki, S.; Tsuruta, M.; Chiba, H. *Nature* **2002**, *415*, 509−511. (b) Kimoto, A.; Masachika, K.; Cho, J. S.; Higuchi, M.; Yamamoto, K. *Org. Lett.* **2004**, *6*, 1179−1182.

(20) Estimated in CH_3CN/CH_2Cl_2 = 1:1. Yamamoto, K.; Higuchi, M.; Kimoto, A.; Imaoka, T.; Masachika, K. *Bull. Chem. Soc. Jpn.* **2005**, *78*, 349−355.

(21) Sun, Y.; Chien, S. C.; Yip, H. L.; Zhang, Y.; Chen, K. S.; Zeigler, D. F.; Chen, F. C.; Lin, B.; Jen, A. K. Y. *Chem. Mater.* **2011**, *23*, 5006−5015.